NASA/TM—2005-213899

Numerical Simulation of the RTA Combustion Rig

Farhad Davoudzadeh
University of Toledo, Toledo, Ohio

Robert Buehrle and Nan-Suey Liu
Glenn Research Center, Cleveland, Ohio

Ralph Winslow
General Electric Aircraft Engines, Cincinnati, Ohio

August 2005

The NASA STI Program Office . . . in Profile

Since its founding, NASA has been dedicated to the advancement of aeronautics and space science. The NASA Scientific and Technical Information (STI) Program Office plays a key part in helping NASA maintain this important role.

The NASA STI Program Office is operated by Langley Research Center, the Lead Center for NASA's scientific and technical information. The NASA STI Program Office provides access to the NASA STI Database, the largest collection of aeronautical and space science STI in the world. The Program Office is also NASA's institutional mechanism for disseminating the results of its research and development activities. These results are published by NASA in the NASA STI Report Series, which includes the following report types:

- TECHNICAL PUBLICATION. Reports of completed research or a major significant phase of research that present the results of NASA programs and include extensive data or theoretical analysis. Includes compilations of significant scientific and technical data and information deemed to be of continuing reference value. NASA's counterpart of peer-reviewed formal professional papers but has less stringent limitations on manuscript length and extent of graphic presentations.

- TECHNICAL MEMORANDUM. Scientific and technical findings that are preliminary or of specialized interest, e.g., quick release reports, working papers, and bibliographies that contain minimal annotation. Does not contain extensive analysis.

- CONTRACTOR REPORT. Scientific and technical findings by NASA-sponsored contractors and grantees.

- CONFERENCE PUBLICATION. Collected papers from scientific and technical conferences, symposia, seminars, or other meetings sponsored or cosponsored by NASA.

- SPECIAL PUBLICATION. Scientific, technical, or historical information from NASA programs, projects, and missions, often concerned with subjects having substantial public interest.

- TECHNICAL TRANSLATION. English-language translations of foreign scientific and technical material pertinent to NASA's mission.

Specialized services that complement the STI Program Office's diverse offerings include creating custom thesauri, building customized databases, organizing and publishing research results . . . even providing videos.

For more information about the NASA STI Program Office, see the following:

- Access the NASA STI Program Home Page at ***http://www.sti.nasa.gov***

- E-mail your question via the Internet to help@sti.nasa.gov

- Fax your question to the NASA Access Help Desk at 301–621–0134

- Telephone the NASA Access Help Desk at 301–621–0390

- Write to:
  NASA Access Help Desk
  NASA Center for AeroSpace Information
  7121 Standard Drive
  Hanover, MD 21076

NASA/TM—2005-213899

Numerical Simulation of the RTA Combustion Rig

Farhad Davoudzadeh
University of Toledo, Toledo, Ohio

Robert Buehrle and Nan-Suey Liu
Glenn Research Center, Cleveland, Ohio

Ralph Winslow
General Electric Aircraft Engines, Cincinnati, Ohio

Prepared for the
40th Combustion, 28th Airbreathing Propulsion, 22nd Propulsion Systems Hazards,
4th Modeling and Simulations Joint Subcommittees Meetings
sponsored by the Joint Army, Navy, NASA, and Air Force Interagency Propulsion Committee
Charleston, South Carolina, June 13–17, 2005

National Aeronautics and
Space Administration

Glenn Research Center

August 2005

Available from

NASA Center for Aerospace Information
7121 Standard Drive
Hanover, MD 21076

National Technical Information Service
5285 Port Royal Road
Springfield, VA 22100

Available electronically at http://gltrs.grc.nasa.gov

Numerical Simulation of the RTA Combustion Rig

Farhad Davoudzadeh
University of Toledo
Toledo, Ohio 43606

Robert Buehrle and Nan-Suey Liu
National Aeronautics and Space Administration
Glenn Research Center
Cleveland, Ohio 44135

Ralph Winslow
General Electric Aircraft Engines
Cincinnati, Ohio 45125

Abstract

The Revolutionary Turbine Accelerator (RTA)/Turbine Based Combined Cycle (TBCC) project is investigating turbine-based propulsion systems for access to space. NASA Glenn Research Center and GE Aircraft Engines (GEAE) planned to develop a ground demonstrator engine for validation testing. The demonstrator (RTA-1) is a variable cycle, turbofan ramjet designed to transition from an augmented turbofan to a ramjet that produces the thrust required to accelerate the vehicle from Sea Level Static (SLS) to Mach 4. The RTA-1 is designed to accommodate a large variation in bypass ratios from sea level static to Mach 4 conditions. Key components of this engine are new, such as a nickel alloy fan, advanced trapped vortex combustor, a Variable Area Bypass Injector (VABI), radial flameholders, and multiple fueling zones. A means to mitigate risks to the RTA development program was the use of extensive component rig tests and computational fluid dynamics (CFD) analysis. This paper summarizes the CFD analytical results of the experimental "Combustion Rig" and the approach is summarized below:

The three-dimensional, compressible, viscous, and turbulent flow characteristics of a variable cycle trapped vortex is simulated via an unstructured and massively parallel, Reynolds-Averaged Navier-Stokes (RANS) code. The computational domain incorporates the Combustion Rig's complex geometry that includes the rectangular duct, a trapped vortex (TV) liner with driver holes, and multiple struts.

A cubic, non-linear low-Reynolds number k-e turbulence model is used. The final grid is an all-hexahedron grid containing approximately 2.2 million elements. The computational results successfully capture the fine details of the complex flow structure such as helical ring vortices, recirculation zones and vortex cores. Consistent with the experimental results, the computational model predicts a major recirculation zone in the trapped vortex cavity region that is protected from the main flow. The trapped vortex can serve as a pilot flame to provide a continuous ignition, helping to keep the flame lit throughout the flight operating envelope. The trapped vortex cavity can significantly enhance mixing.

Experimental and computational tests are performed to establish the correlation between pressure ratio and the mass flow rate through the trapped vortex driver holes. The vortex structure relative to this pressure ratio is presented.

Introduction

The Revolutionary Turbine Accelerator (RTA)/Turbine Based Combined Cycle (TBCC) project sponsored by the NASA Glenn Research Center (GRC) has been investigating turbine-based propulsion systems for access to space (ref. 1). Turbine propulsion provides the potential for aircraft-like, space-launch operations that may significantly reduce launch costs and improve safety. During this initial phase of RTA/TBCC, NASA GRC along with General Electric Aircraft Engines (GEAE), has designed a ground demonstrator engine for validation testing. This ground demonstrator engine is designated as RTA-1 and was scheduled to be tested in 2006.

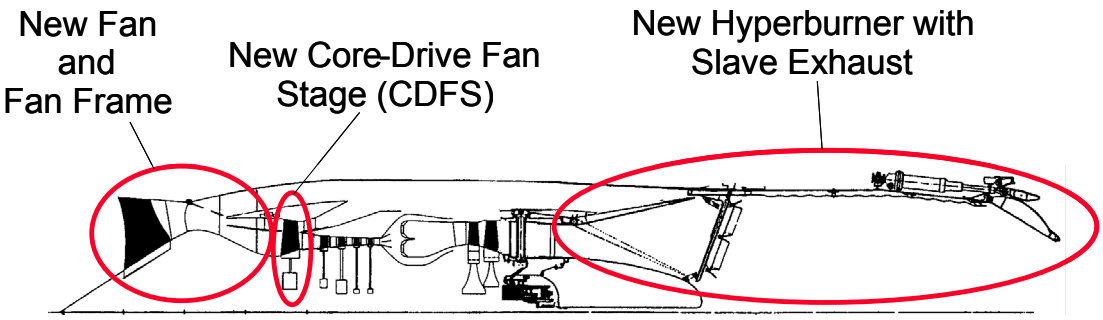

Figure 1.—RTA-1 Mach 4+ Demonstrator Engine Definition.

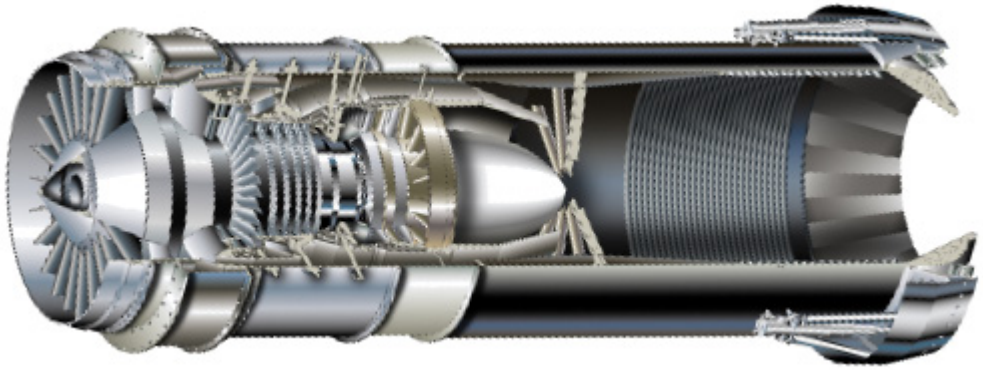

Figure 2.—RTA-1 Engine Concept.

The demonstrator is a turbofan ramjet combined cycle engine, designed to transition from an augmented turbofan to a ramjet for peak thrust performance throughout the acceleration mission to Mach 4+. GEAE will use an existing YF120 engine core integrated with new components in the demonstration of this low-cost, versatile, Mach 4+ demonstrator (figs. 1 and 2). The RTA-1 incorporates a new fan and new core drive fan stage (CDFS), and material upgrades to the YF120 stage 2 and 3 compressor to withstand the elevated temperatures at the higher Mach engine conditions. A new hyperburner (augmentor/ramjet) was developed along with an axisymmetric slave nozzle.

RTA-1 OPERATION

The RTA-1, a turbofan ramjet, is designed to produce the required thrust to provide acceleration throughout the flight envelope from Sea Level Static to Mach 4+. The specific test points that are critical to the flight demonstration are listed below (fig. 3):

- Take-off
- Double bypass mode transition
- Ramjet mode transition
- Transonic acceleration
- Mach 4+ operation
- Windmilling at high Mach (core-on and core-off)

The variable-cycle RTA-1 allows for high fan pressure ratio mode for sea level static (SLS) to Mach 2 flight speeds, and transitions to a lower fan pressure ratio mode for operation up to Mach 3. Above

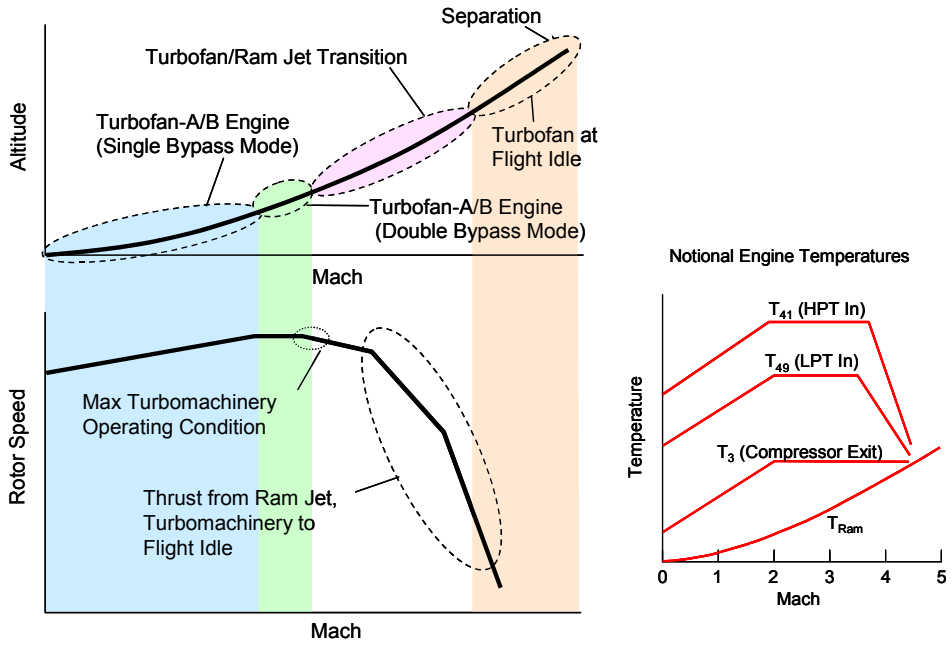

Figure 3.—RTA-1 Operation and Basic Engine Operating Temperatures.

Mach 3, the hyperburner transitions from a conventional augmentor to a ramjet burner, accelerating the vehicle to Mach 4+. During this acceleration from Mach 3 to 4+, the turbomachinery is brought back to flight-idle speeds. The turbomachinery is not completely shut down during this acceleration, so air restarts are not required in TSTO vehicles after separation of the second stage.

Key Technical Issues

A number of technical challenges require careful attention during the RTA-1 design process. The fan, core, and hyperburner must match over a wide range of fan and core energy with acceptable hyperburner performance. Transition from an augmented to ramjet mode requires a sophisticated fuel and hyperburner system. Also, high-Mach inlet temperatures necessitate thermal management systems to protect structures and bearings.

The TSTO mission profile requires a 10X swing in bypass ratio (BPR) between the core and bypass flow to achieve engine operation from takeoff to Mach 4+. This is achieved with the addition of a new fan and CDFS that combine to provide a lower overall pressure ratio compared to the YF120 engine. Also, new and existing variable geometry combine to adjust the flow split between the fan and core streams to match the hyperburner inlet requirements. The combination of fan and variable geometry operating characteristics provides the required flexibility in design for the TSTO mission.

The hyperburner operates over the entire TSTO mission to vehicle separation. At takeoff, most of the air delivered to the hyperburner comes from the core stream. At Mach 4+ operation, most of the air comes from the fan stream. Movement of the variable-area bypass injector and fueling of the hyperburner must allow smooth operation throughout the wide range of conditions. GEAE performed extensive component rig tests to develop a database for designing the RTA-1 engine hardware.

Combustion Rig Description

The Combustion Rig (fig. 4.) is the test hardware that was developed to reduce risk to the RTA-1 engine demonstrator. The Combustion Rig is water cooled, atmospheric pressure rig, with a rectangular

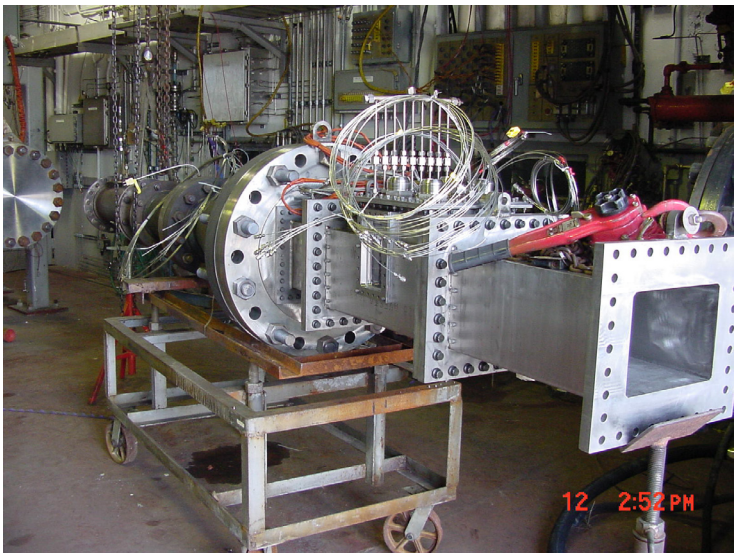

Figure 4.—Combustion Rig Being Installed into the GE Facility.

cross section. The rig inlet temperature is controlled by a vitiated in-line combustor that can provide air flow up to a maximum of 1600 °F or by a non-vitiated facility heater up to a maximum temperature of 1200 °F. The inlet temperatures are set to match the flight demonstration conditions within the limits of the facility. The mass flow rate is adjusted to provide the relative Mach numbers to simulate the targeted engine condition. The air supply to the trapped vortex is controlled separately at various pressure ratios. The trapped vortex geometry is approximately full scale to the engine hardware.

A variety of trapped vortex designs were investigated with the Combustion Rig, as well as a multitude of fueling schemes. The work of Roquemore, et. al. (ref. 2) and the TV Combustor work at GE were leveraged heavily in the design of the trapped vortex geometries (fig. 5). The understanding of the complex behavior in the trapped vortex over a wide range of expected pressure ratios in the RTA cycle was a primary goal of the CFD work that was performed by NASA. The primary function of the trapped vortex is to provide a protected sight from the main flow stream for fuel injection and ignition in the TV and the circumferential propagation of this ignition source. Another important design consideration is the flame spreading from the cavity. This paper presents the CFD calculation made of the Combustion Rig geometry. The CFD calculations were used to validate non-reacting test results and to get a better insight into the complex flow structure developed in the trapped vortex. A key parameter that was investigated was the sensitivity of the pressure ratio across the air driven trapped vortex and the associated flow structure in the cavity. The Sea Level Static flight condition was selected for the CFD calculations as this condition is the most severe temperature condition.

Computational Method

The computational work performed to produce the numerical results presented in this paper uses the National Combustion Code (NCC), developed at NASA Glenn Research Center (GRC) for comprehensive modeling and simulation of aerospace combustion systems.

The focus in the development of the integrated system of computer codes has been to calculate the fluid, thermal, and chemical characteristics of real-world combustors to an appropriate level of accuracy and turnaround time desired by designers and analysts. The two foremost important obstacles to turnaround time have been grid generation and serial processing.

Use of unstructured or overset grids and parallel computing minimizes the overall time needed to achieve a numerical solution. Thus the main focus has been to incorporate a numerical scheme that

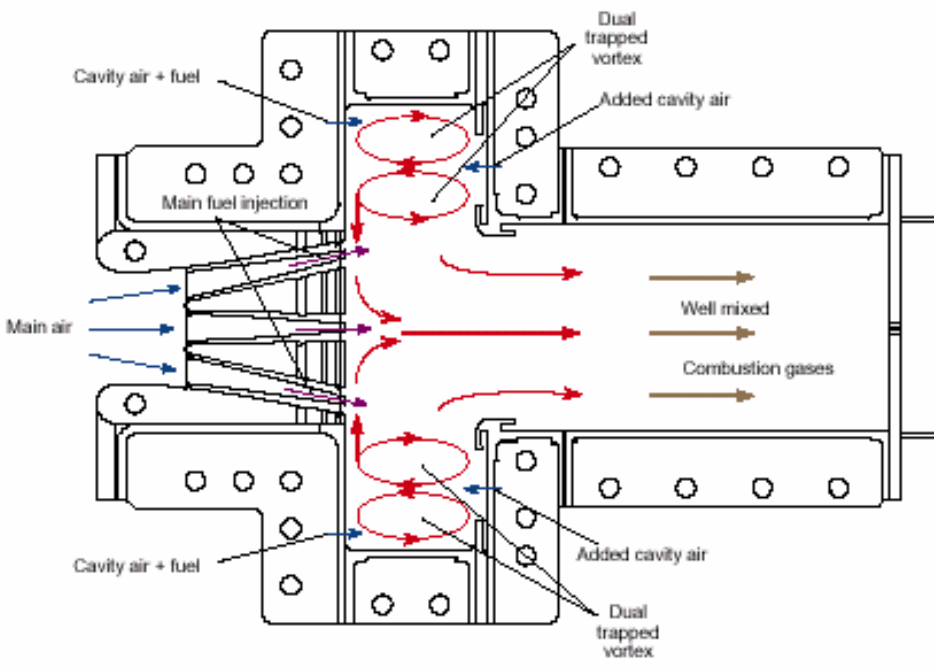

Figure 5.—Illustration of a Trapped Vortex Combustor.

allows use of a large number (thousands) of processors in parallel to shorten the solution time and to provide speed-ups that does not deteriorate with the addition of more processors.

The main flow solver for the code used in this work is based on an explicit four-stage Runge-Kutta scheme, which is very suitable for parallelization. Figure 6 shows an example of the speedup that has been achieved with the code on an SGI Origin 2000 (ref. 3). This 3-D test case uses 1.3 million tetrahedral elements for simulation of a premixed hydrogen/air combustor (ref. 4), using the Intrinsic Low Dimensional Manifold (ILDM) kinetics module (refs. 5 and 6). The parallel speedup metric is calculated by taking the ratio of the time per iteration for the serial case versus the time per iteration for the parallel case. The parallel efficiency is the ratio of the parallel speedup to the number of processors used in the calculation. Davoudzadeh, et. al. (ref. 7) reported a factor of two speedup for a 2.5 million elements domain when they increased the number of processors from 200 to 400.

To facilitate the grid generation task, the code is designed to use unstructured meshes. It uses triangular and/or quadrilateral elements in the 2-D cases, and tetrahedrons, wedges, pyramids, and hexahedrons in the 3-D cases. A combination of these grid types can be used to create hybrid grids. For example, to resolve the boundary layer one may choose to use hexahedron elements in the wall region and transition out of the boundary layer to tetrahedron elements via pyramid elements.

In brief, the flow solver solves unsteady, 3-D, compressible Navier-Stokes equations. The discretization begins by dividing the computational domain into a large number of elements, which can be of mixed types. A central-difference finite-volume scheme augmented with numerical dissipation is used to generate the discretized equations, which are then advanced temporally by an explicit 4-stage Runge-Kutta scheme. For low Mach number compressible flow, a pre-conditioning is applied to the governing equations, and the solution is advanced temporally by a so-called “dual-time-step” approach, in which the Runge-Kutta scheme is used for the “inner” iteration. The turbulence model used in the present work is a cubic non-linear k-epsilon mode (ref. 8) with low Reynolds number wall integration. This turbulence model is reported (ref. 8) to capture the recirculation zones and their structures with more accuracy, relative to the standard k-epsilon model. A description of the solver and some benchmark test cases can be found in references 9 and 10.

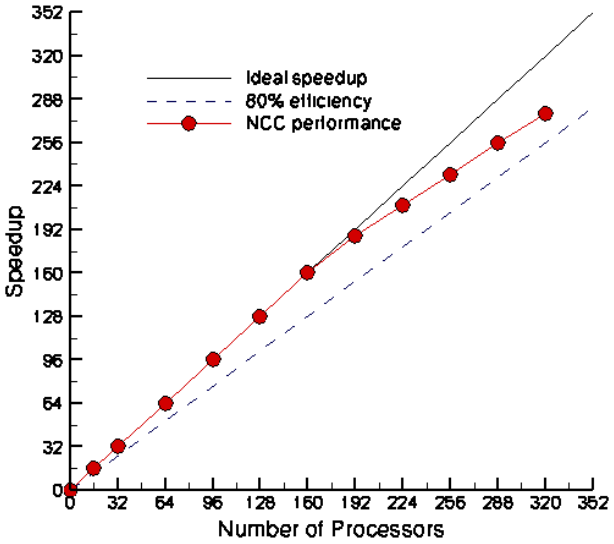

Figure 6.—Speedup curve for the 1.3 M element test case (ref. 3).

Experimental Setup and the Geometry

The experimental setup for the rig is shown in figure 4. For the computational work, two different geometries were used. The first geometry shown in figure 7, is used for the flowcheck calculations. This geometry does not include any internal appendages and is used to validate the computational code. The second geometry, shown in figure 8, is more complex and contains seven flowbars located farthest upstream, three additional flowbars upstream, and three struts used as bluff bodies. The flowbars are intended for fueling the rig. The struts are used to create low pressure zones where vortical structures are created and sustained, as will be shown later.

The Computational Grid

The computational grids for both geometries are created using the Gridgen software. Both grids consists of all hexahedron elements. A total of 1,119,730 and 2,201,214 hexahedron-only elements are used for creating the flowcheck grid and the combustion rig full grid respectively. Figure 9 shows the grid distribution used for the flowcheck calculations.

In contrast to grid topologies where the centerline becomes the axis of singularity around which wedge type elements are generated, in these all-hexahedron mesh, there is no axis of singularity (see fig. 10).

Computational Results

All the cases for which a numerical simulation is performed are shown in table 1. The first two cases (flowcheck) are used for validating the computational code. General Electric Aircraft Engines performed experiments for these two cases where they measured the mass flowrates through the driver holes (shown in figs. 8 and 9). These measured mass flow rates are to be compared with the simulated results to provide confidence in the ability of the code to predict the flow.

The “Test Conditions” calculations are performed for the full geometry shown in figure 8. The only difference between these two cases is the value of the ratio of the inlet total pressure (Pt) applied on the driver holes, to the static pressure at the exit. The final case is for the engine condition where the back pressure and the total inlet temperature is significantly higher than those applied in the test conditions, as shown in the table 1.

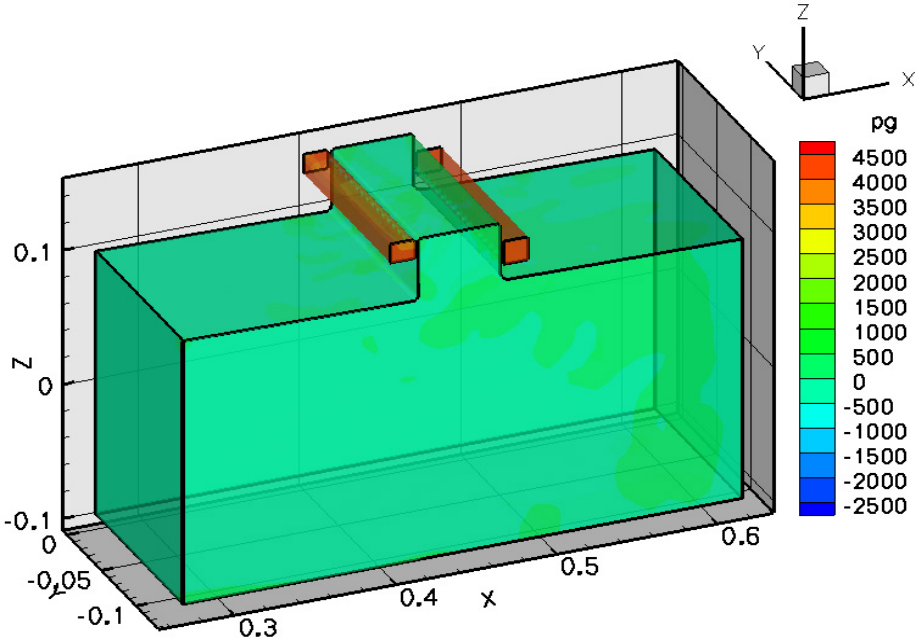

Figure 7.—Geometry used for the flowcheck calculations.

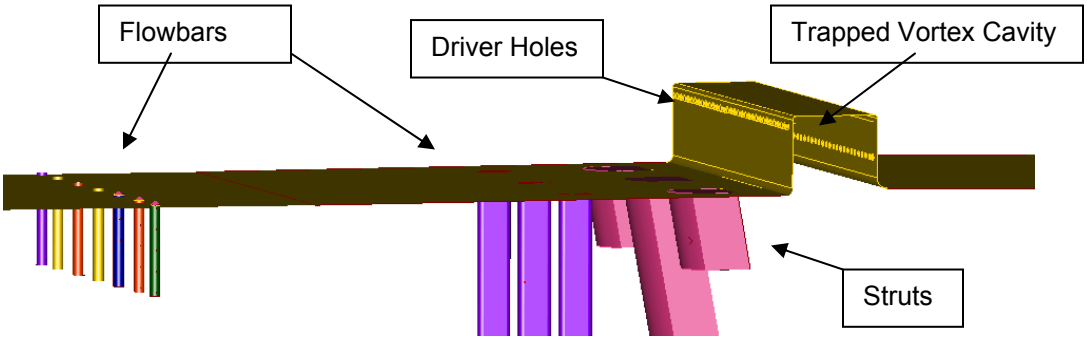

Figure 8.—Combustion Rig full geometry.

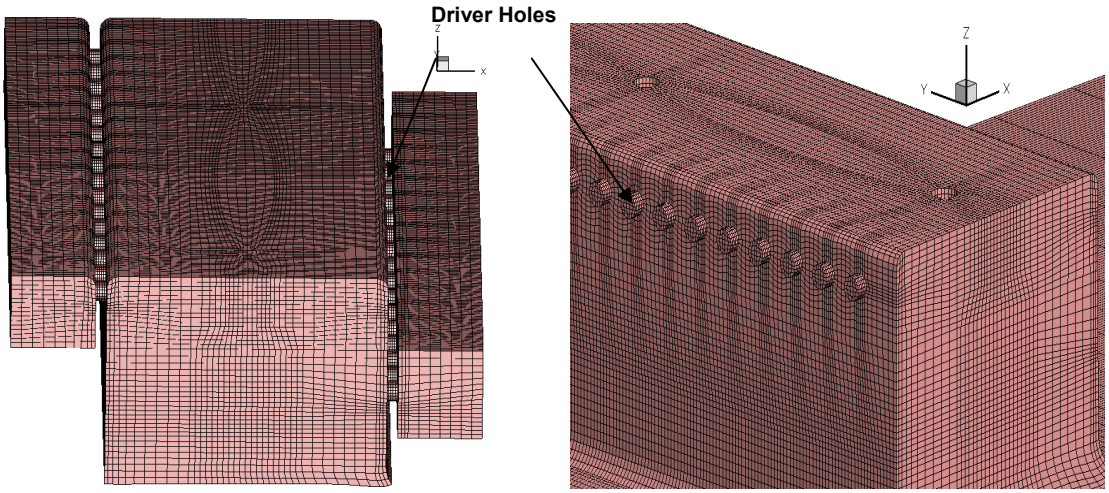

Figure 9.—Grid distribution on the trapped vortex cavity and on the driver holes.

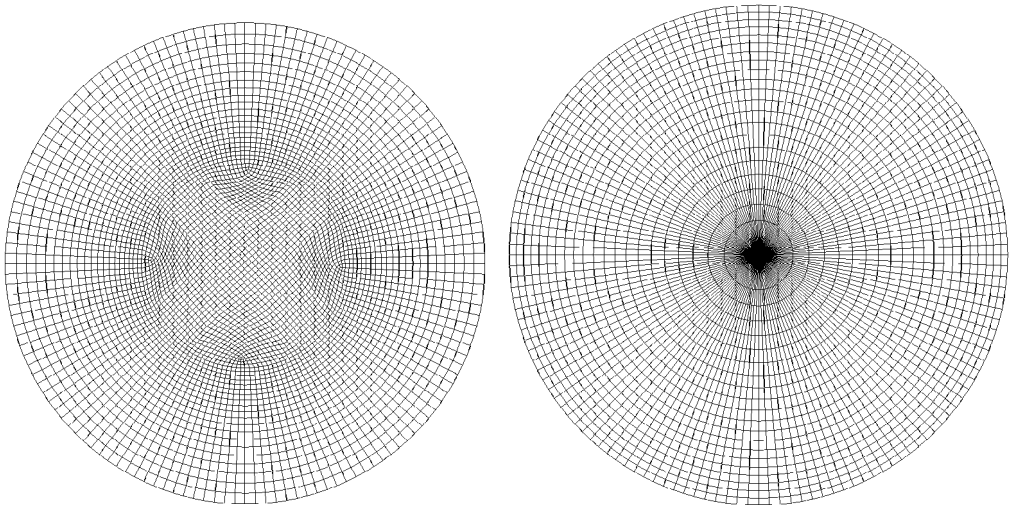

Figure 10.—Centerline region grid topologies.

TABLE 1.—COMPUTATIONAL CASES CONSIDERED

CASE	Description	Back Pressure (Ps)	Trapped Vortex Pt/Ps	Temp. (Kelvin)
Flow Check (1)	No Struts, No Flow Bars	101,325.0 Pa	1.04	Tt, Driver-holes: 294
Flow Check (2)	No Struts, No Flow Bars	101,325.0 Pa	1.10	Tt, Driver-holes: 294
Test Condition (1)	Full Geometry Sea Level Static	101,325.0 Pa	1.04	Tt, Driver-holes: 294 Ts, Core: 811
Test Condition (2)	Full Geometry Sea Level Static	101,325.0 Pa	1.10	Tt, Driver-holes: 294 Ts, Core: 811
Engine Condition	Full Geometry Sea Level Static	273,026.0 Pa	1.14	Tt, Driver-holes: 461 Ts, Core: 1306

The Flowcheck Results

The boundary conditions used for the flowcheck calculations are shown in figure 11. In the transverse direction, a plane of symmetry boundary condition is applied on one side and the wall on the other side. The inlet boundary condition is applied to the two faces of the boxes attached to the sixty four driver holes. This will allow for non-uniform pressure distribution on each hole. The non-uniform pressure distribution on each hole will emerge due to the development of the vortical structures inside the vortex cavity.

Figure 12 shows the particle traces in the cavity, demonstrating the flow structure predicted by the numerical simulation. The traces are colored by the value of the streamwise component of the velocity. Figure 13 shows particle traces at a particular cross section for two different pressure ratios. Clearly, the particle traces for the pressure ratio of 1.10 show a stronger vortical structure that protrudes outside of the cavity.

Comparisons of the measured mass flow rates and the computed mass flow rates are shown in table 2. The comparison for the pressure ratio of 1.1 shows exact one to one prediction. This is not so for the lower pressure ratio of 1.04. This may be due to inaccuracies in the facility flow measurement device at the lower flowrates.

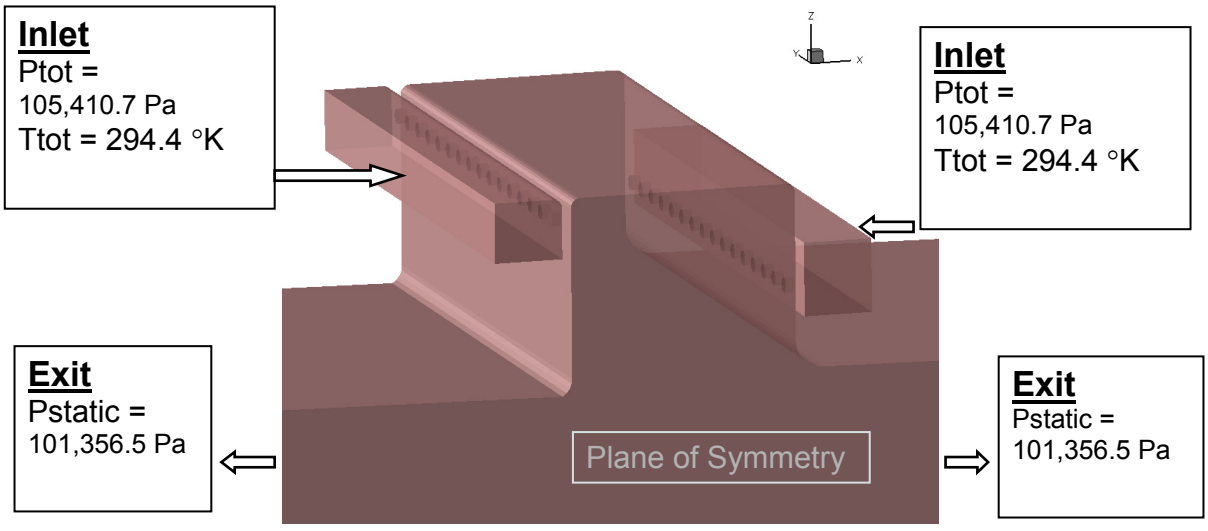

Figure 11.—Boundary conditions for the “Flowcheck” calculations.

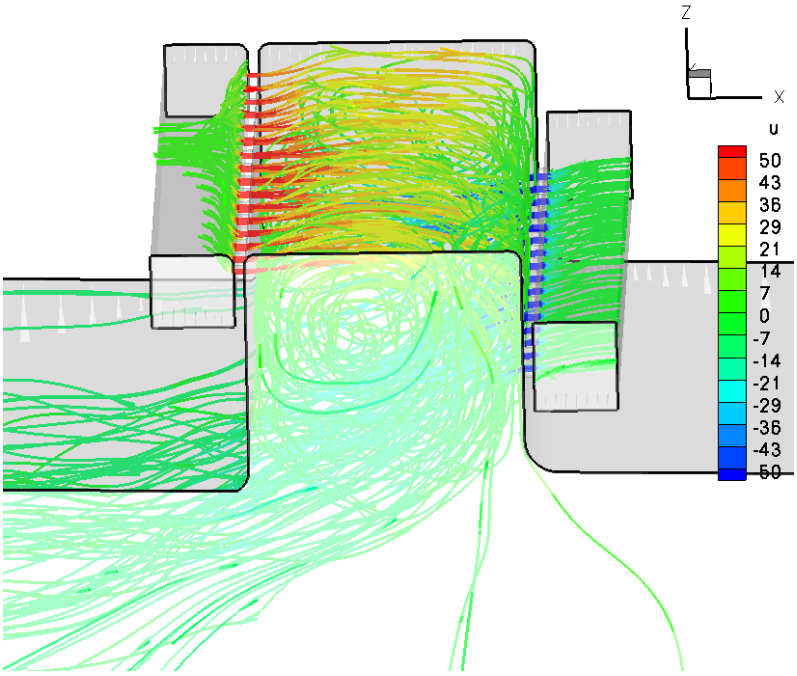

Figure 12.—Particle traces showing the vortical structure inside the trapped vortex cavity.

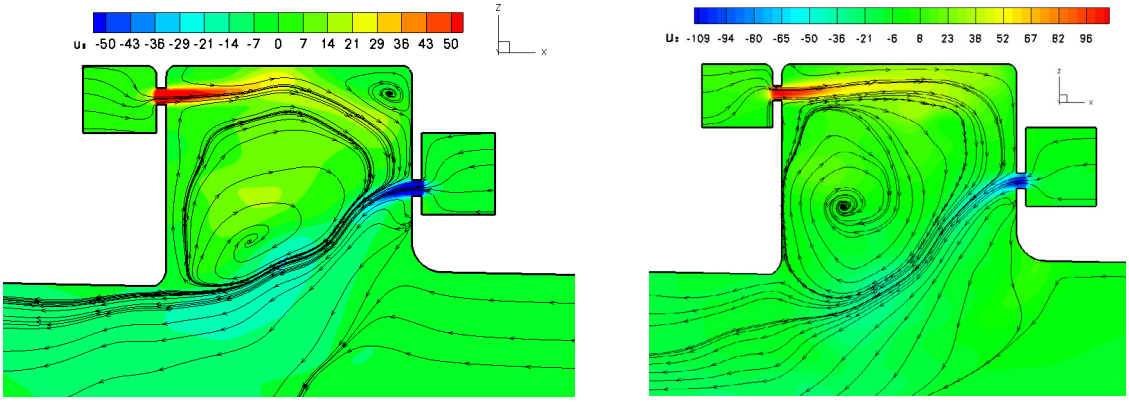

Pressure Ratio = 1.04, Y-const = –0.05 **Pressure Ratio = 1.10, Y-const = –0.05**

Figure 13.—Contours of u-velocity and the particle traces for the two pressure ratios.

TABLE 2.—COMPARISON OF THE COMPUTED RESULTS AND THE EXPERIMENTAL MEASUREMENTS

CASE	Description	Trapped Vortex Pt/Ps	Normalized Measured Mass Flow rate Through Driver-Holes	Normalized Computed Mass Flow rate Through Driver-Holes
Flow Check (1)	No Struts, No Flow Bars	1.04	1.0	1.2
Flow Check (2)	No Struts, No Flow Bars	1.10	1.58	1.58

Test Conditions and the Engine Condition Results

Figure 14 shows particle traces colored by the value of the streamwise velocity and demonstrates the general three-dimensional features of the computed flow field. The vortical structures created inside the trapped vortex are ingested into the low pressure 'wells' generated aft of the bluff bodies (i.e., struts) shown in figure 8. Inside the trapped vortex, the flow swirls from the walls towards the centerline. On it's path it encounters the low pressure regions created by the struts and consequently flows inside these low pressure regions and down the struts, and eventually downstream. The low pressure recirculation zones aft of the struts create an ideal environment for mixing of the air and the fuel and act to produce a very stable flame.

Figure 15 shows the cross sections at various transverse locations. Each cross section shows axial-velocity distribution, as well as the particle traces.

The cross-section A is closest to the wall. There are two distinct recirculation zones shown in this cross section. Cross-section B is farther away from the wall and contains the first strut. The structure of the particle traces shows that the flow is ingested in the low pressure vacuum created aft of the strut. Further, the flow continues to recirculate aft of the bluff body. This situation, as mentioned before, will force the mixing of the oxidants and the fuel and can create a stable recirculation zone where in a reacting flow would lead to a stable flame that can act as a pilot. Cross-section C is inside the cavity and does not include any of the internal appendages. In this section the swirling flow is contained in the tapped vortex cavity and creates two very strong recirculation zones. Similarly cross-section D shows several recirculation zones of different strengths inside the cavity. The cross-section E, again shows how the flow is ingested inside the low pressure region aft of the second strut.

Figure 16 shows cross-sections at the same location for the three different pressure ratios. At test condition (1) where the pressure ratio is 1.04, there is only one relatively large counter-clockwise recirculation zone. At test condition (2) the recirculation zone becomes tighter and a second clockwise recirculation zone on the left and just below the driver holes is beginning to emerge. At the engine condition there are two dense recirculation zones inside the trapped vortex cavity. It should be noticed that these particle traces are projected to a plane, and in reality they are three-dimensional with a helical shape swirling from one end to the other, as shown earlier in figure 14.

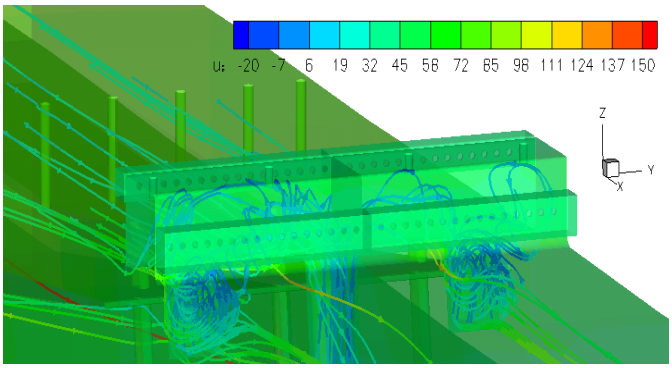

Figure 14.—Recirculation zones aft of the struts at pressure ratio = 1.14

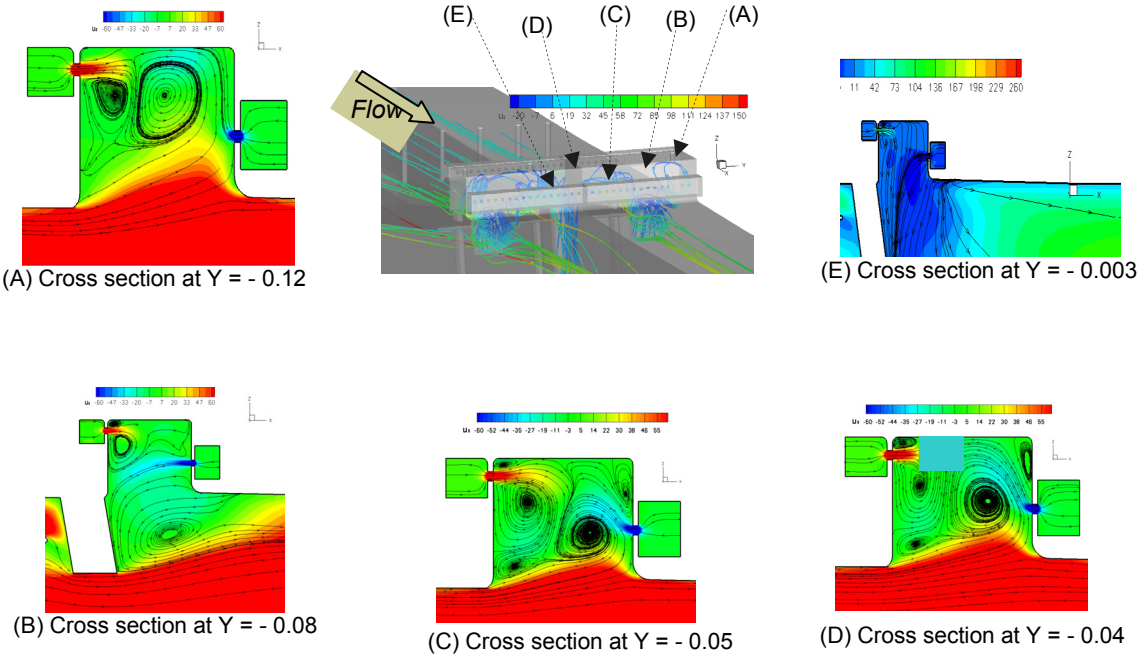

Figure 15.—Perspective view of the flow field and the associated cross-sections pressure ratio = 1.14

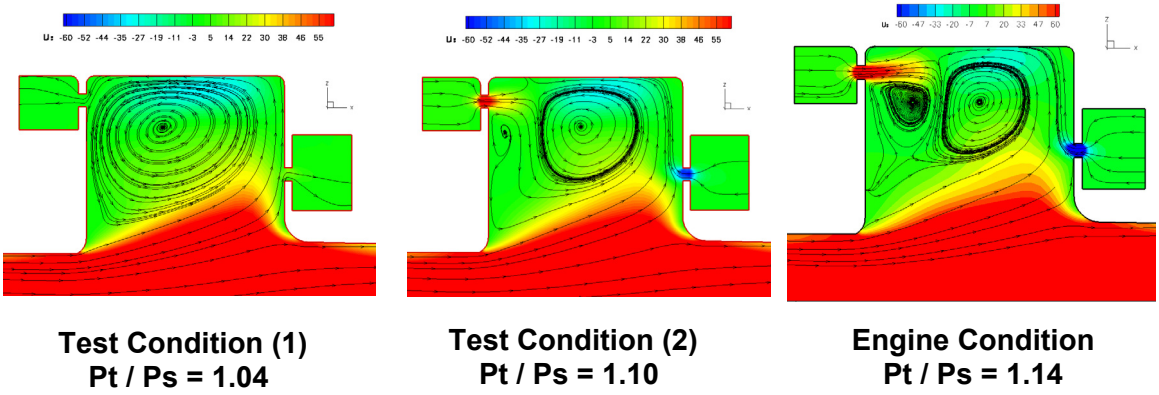

Figure 16.—Cross-sections at y = –0.118 for three different operating conditions showing u-velocity contours and particle traces.

Figure 17 shows cross-sections at a location which includes one of the struts. These sections show how the flow is ingested inside of the low pressure zones aft of the bluff bodies. The shape and strength of the recirculation zones downstream of the struts is a function of the flow in the main core. The flow Mach number in the main core for the test conditions is almost identical; what sustains a stronger recirculation zone for the pressure ratio of 1.10, relative to “Test Condition (1),” is simply the higher pressure ratio. In the case of the “Engine Condition,” the core static pressure is higher and the pressure ratio is also higher, which causes the recirculation zones to be more expanded. Furthermore, the secondary recirculation zone inside the cavity just aft of the driver holes is still present. Figures 18 and 19 are similar cross-sections at different spanwise locations.

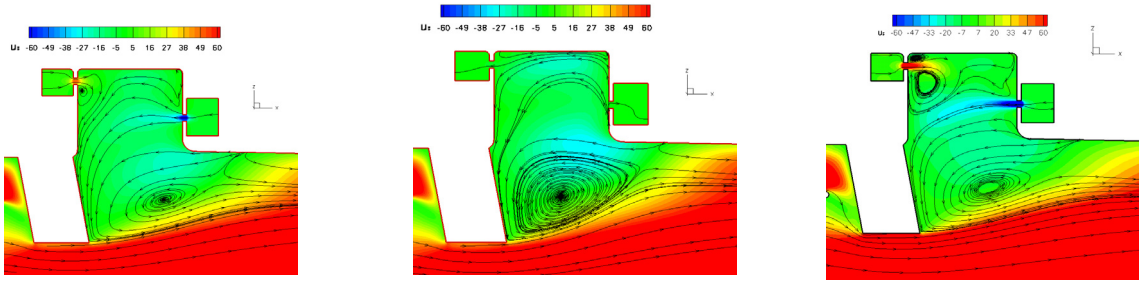

Test Condition (1)
Pt / Ps = 1.04

Engine Condition
Pt / Ps = 1.14

Figure 17.—Cross-sections at y = –0.0875 for three different operating conditions showing u-velocity contours and particle traces.

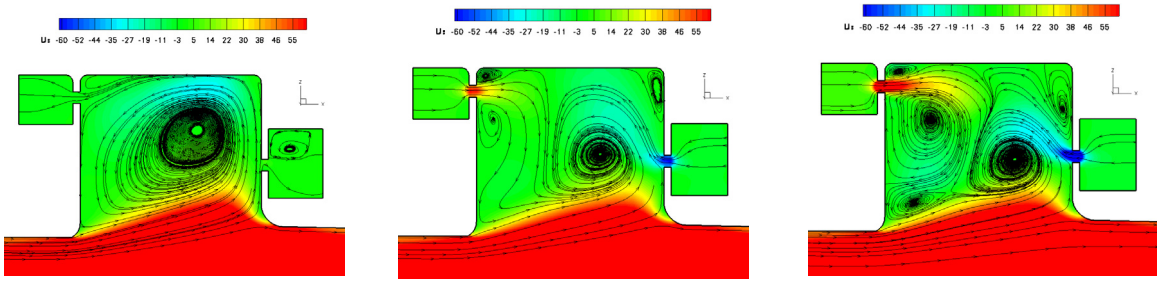

Test Condition (1)
Pt / Ps = 1.04

Test Condition (2)
Pt / Ps = 1.10

Engine Condition
Pt / Ps = 1.14

Figure 18.—Cross-sections at y = –0.05 for three different operating conditions showing u-velocity contours and particle traces.

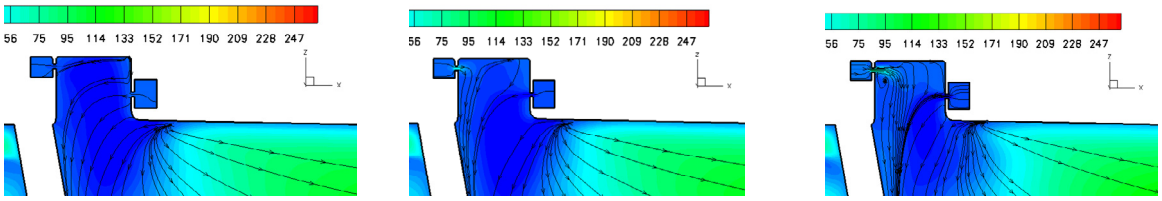

Test Condition (1)
Pt / Ps = 1.04

Test Condition (2)
Pt / Ps = 1.10

Engine Condition
Pt / Ps = 1.14

Figure 19.—Cross-sections at y = –0.003 for three different operating conditions showing u-velocity contours and particle traces.

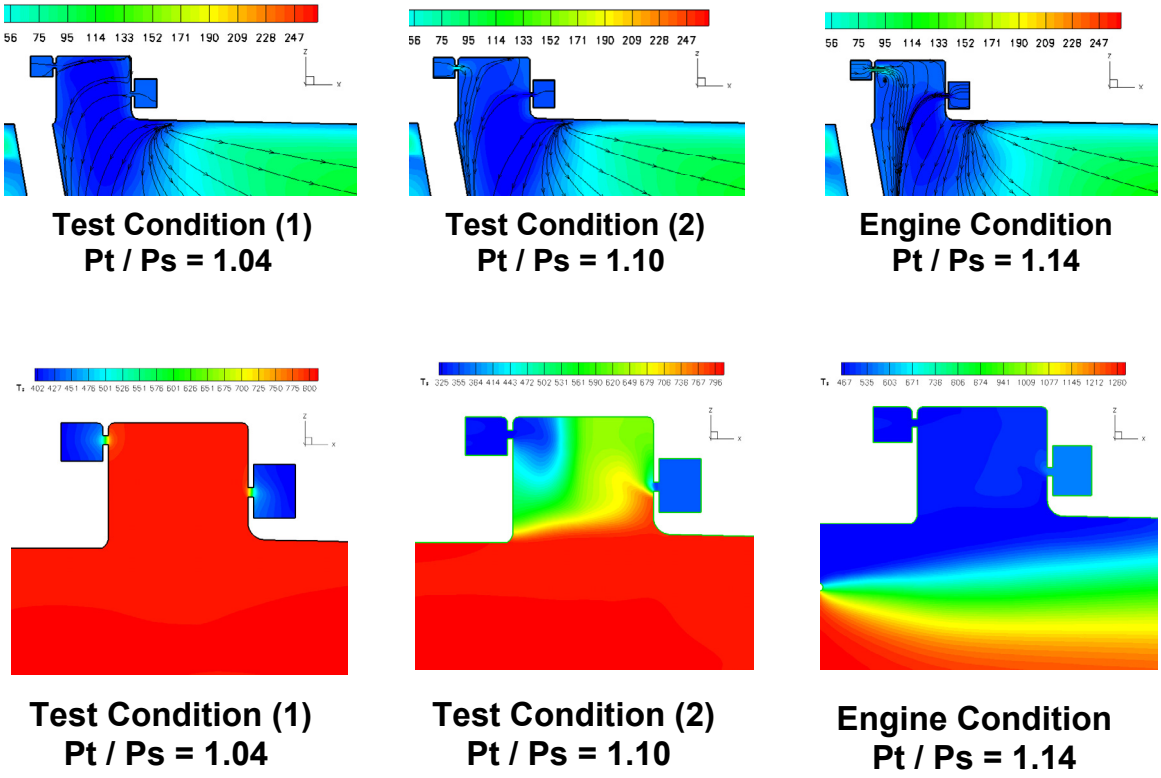

Figure 20.—Cross-sections at y = –0.05 for three different operating conditions showing static temperature contours.

Figure 20 shows cross-sections of the static temperature distribution. These distributions demonstrate the degree of mixing of the core flow and the flow coming through the driver holes. It is evident that for the "Test Condition (1)" the core flow has fully penetrated the trapped vortex cavity. In the case of "Test Condition (2)," due to the higher pressure ratio, there is better penetration of the flow through the driver holes into the cavity. In the case of the "Engine Condition," the inner portion of the duct is at a higher temperature than the outer portion of the duct. The temperature mixing of these separate flow streams is observed.

Conclusions

An experimental model combustion rig containing a trapped vortex feature is numerically modeled to support the design of a Turbine Based Combined Cycle Engine (TBCC)/Revolutionary Turbine Accelerator (RTA), and to demonstrate the modeling capabilities of a computer code in predicting the flow characteristics of these combustors.

To minimize the overall turnaround time, unstructured grids are used for the discretization of the partial differential equations and parallel computing system is employed to perform the calculations. The numerical simulation solves RANS equations together with a cubic, non-linear k-epsilon turbulence model.

The simulation is conducted for various pressure ratios for the flowcheck geometry as well as the full geometry, encompassing a set of ten upstream flow-bars, three hanging struts, sixty four driver holes and a trapped vortex cavity.

The simulation captured details of the flowfield associated with this combustor. An important feature predicted is the creation of the swirling vortical flow inside the trapped vortex cavity and its interaction with the struts located in the main core region. The predictions showed that the swirling flow from the trapped vortex region is ingested into the the low pressure regions created aft of the struts where the flow

continues to recirculate and creates a stable recirculation zone ideal for the mixing of the reactants. These stable recirculation zones can serve to maintain a stable flame in these regions.

Comparisons of the computed mass flowrate through the driver holes with the experimental data showed good agreement.

References

1. Shafer, D.G., and McNelis, N., "Development of a Ground Based Mach 4+ Revolutionary Turbine Accelerator Technology Demonstrator (RTATD) for Access to Space" ISOABE 2003.
2. Roquemore, W.M., et. al., "Trapped Vortex Combustor Concept for Gas Turbine Engines," AIAA Paper 2001–0483.
3. Quealy, A., 2002, "National Combustion Code Parallel Performance Enhancements," AIAA Paper no. 2002–3706.
4. Shih, T.-H., Norris, A., Iannetti, A., Marek, J., Liu, N.-S., Smith, T., Povinelli, L.A., (2001), "Study of Hydrogen/Air Combustor Using NCC," AIAA Paper no. 2001–0808.
5. Norris, A.T., 1997, "Automated Simplification of Full Chemical Mechanisms, AIAA Paper no. 97–3115.
6. Norris, A.T., 1998, "Automated Simplification of Full Chemical Mechanisms—Implementation in National Combustion Code," AIAA Paper no. 98–3987.
7. Davoudzadeh, F., and Liu, N.S.,: "Numerical Prediction of Non-reacting and Reacting Flow in a Model Gas Turbine Combustor," Proceedings of ASME Turbo Expo 2004, Power for Land, Sea, and Air, June 14–17, 2004, Vienna, Austria.
8. Shih, T.-H., Chen, K.-H., and Liu, N.S., 1998, "A Non-Linear K-epsilon Model for Turbulent Shear Flows," AIAA Paper 98–3983.
9. Liu, N.-S., "On the Comprehensive Modeling and Simulation of Combustion Systems," AIAA–2001–0805, 39th AIAA Aerospace Sciences Meeting & Exhibit, 8–11 January 2001/Reno, NV. Ryder, R.C., "The Baseline Solver for the National Combustion Code," AIAA Paper 98–3853, July 1998, Cleveland, OH.

REPORT DOCUMENTATION PAGE

Form Approved
OMB No. 0704-0188

1. AGENCY USE ONLY (*Leave blank*)	2. REPORT DATE	3. REPORT TYPE AND DATES COVERED
	August 2005	Technical Memorandum

4. TITLE AND SUBTITLE

Numerical Simulation of the RTA Combustion Rig

5. FUNDING NUMBERS

WBS–22–714–02–20

6. AUTHOR(S)

Farhad Davoudzadeh, Robert Buehrle, Nan-Suey Liu, and Ralph Winslow

7. PERFORMING ORGANIZATION NAME(S) AND ADDRESS(ES)

National Aeronautics and Space Administration
John H. Glenn Research Center at Lewis Field
Cleveland, Ohio 44135–3191

8. PERFORMING ORGANIZATION REPORT NUMBER

E–15270

9. SPONSORING/MONITORING AGENCY NAME(S) AND ADDRESS(ES)

National Aeronautics and Space Administration
Washington, DC 20546–0001

10. SPONSORING/MONITORING AGENCY REPORT NUMBER

NASA TM—2005-213899

11. SUPPLEMENTARY NOTES

Prepared for the 40th Combustion, 28th Airbreathing Propulsion, 22nd Propulsion Systems Hazards, 4th Modeling and Simulations Joint Subcommittees Meetings sponsored by the Joint Army, Navy, NASA, and Air Force Interagency Propulsion Committee, Charleston, South Carolina, June 13–17, 2005. Farhad Davoudzadeh, University of Toledo, 2801 W. Bancroft Street, Toledo, Ohio 43606; Robert Buehrle and Nan-Suey Liu, NASA Glenn Research Center; and Ralph Winslow, General Electric Aircraft Engines, One Neumann Way, Cincinnati, Ohio 45125. Responsible person, Farhad Davoudzadeh, organization code RTB, 216–433–8876.

12a. DISTRIBUTION/AVAILABILITY STATEMENT

Unclassified - Unlimited
Subject Categories: 01, 05, 07, and 31

Available electronically at http://gltrs.grc.nasa.gov

This publication is available from the NASA Center for AeroSpace Information, 301–621–0390.

12b. DISTRIBUTION CODE

13. ABSTRACT ***(Maximum 200 words)***

The Revolutionary Turbine Accelerator (RTA)/Turbine Based Combined Cycle (TBCC) project is investigating turbine-based propulsion systems for access to space. NASA Glenn Research Center and GE Aircraft Engines (GEAE) planned to develop a ground demonstrator engine for validation testing. The demonstrator (RTA-1) is a variable cycle, turbofan ramjet designed to transition from an augmented turbofan to a ramjet that produces the thrust required to accelerate the vehicle from Sea Level Static (SLS) to Mach 4. The RTA-1 is designed to accommodate a large variation in bypass ratios from sea level static to Mach 4 conditions. Key components of this engine are new, such as a nickel alloy fan, advanced trapped vortex combustor, a Variable Area Bypass Injector (VABI), radial flameholders, and multiple fueling zones. A means to mitigate risks to the RTA development program was the use of extensive component rig tests and computational fluid dynamics (CFD) analysis.

14. SUBJECT TERMS

Trapped vortex; Flameholder; RAVS; Liquid jet-A; Combustion; Revolutionary turbine accelerator

15. NUMBER OF PAGES

21

16. PRICE CODE

17. SECURITY CLASSIFICATION OF REPORT	18. SECURITY CLASSIFICATION OF THIS PAGE	19. SECURITY CLASSIFICATION OF ABSTRACT	20. LIMITATION OF ABSTRACT
Unclassified	Unclassified	Unclassified	